

Sesquiterpenoids from *Incarvillea arguta*: Absolute Configuration and Biological Evaluation

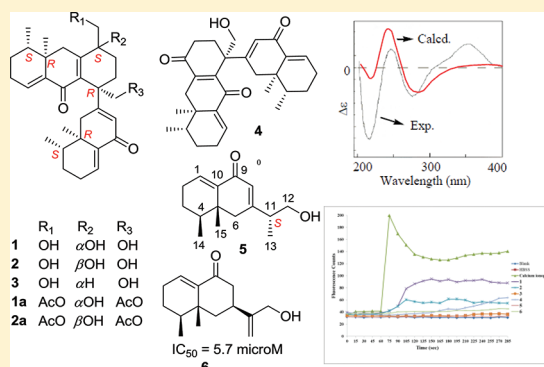
Yong-Ming Yan,^{†,‡} Gui-Sheng Wu,[†] Xiao-Ping Dong,[‡] Lan Shen,[†] Yan Li,[†] Jia Su,[†] Huai-Rong Luo,[†] Hua-Jie Zhu,^{*,†} and Yong-Xian Cheng^{*,†,‡}

[†]State Key Laboratory of Phytochemistry and Plant Resources in West China, Kunming Institute of Botany, Chinese Academy of Sciences, Kunming 650204, People's Republic of China

[‡]College of Pharmacy, Chengdu University of Traditional Chinese Medicine, Chengdu 610075, People's Republic of China

S Supporting Information

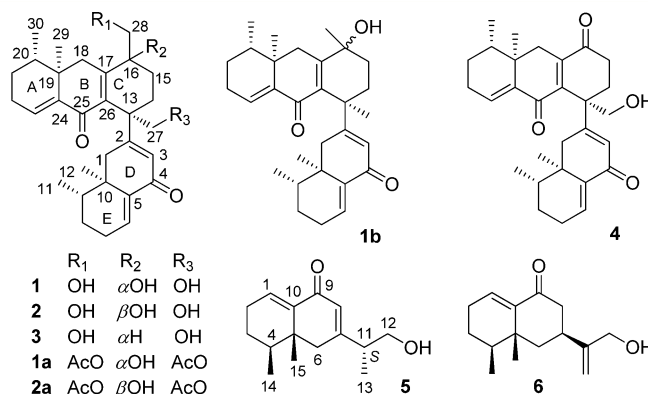
ABSTRACT: Diincarvilones A–D (1–4), incarvilone A (5), and a known compound, argutosine B (6), were isolated from *Incarvillea arguta*. The structures, including the absolute configurations of the new compounds, were determined by NMR spectroscopy, X-ray diffraction analysis, CD spectroscopy, and a variety of computational methods. The biological properties of these substances, including effects on intracellular Ca²⁺ influx, nitric oxide (NO) production, and human cancer cells, were evaluated. The results showed that at the concentration of 10 μM (in HBSS buffer) diincarvilones A and B cause a persistent increase in cytoplasmic calcium levels in A549 cells.



The genus *Incarvillea* comprises 15 species worldwide, 11 of which are found in China.¹ The documented effects of *Incarvillea* plants on pain, inflammation, rheumatism, and weakness have motivated a number of studies that have characterized the chemical constituents of this genus.^{2,3} *I. arguta* is an ethnobotanical herb in China used to treat hepatitis, nephritis, and cancer,⁴ and it has aroused significant interest in the past.⁵ During our search for bioactive compounds from traditional medicine based on ethnopharmacological knowledge, four new sesquiterpenoids (1–4), which possess an unusual hydrodecalenone-substituted tricyclic skeletal framework, along with one new and one known sesquiterpenoid, were isolated. Thus far, only two sesquiterpenoid analogues of compounds 1–4 have been characterized from the plants of the genus *Eremophila*.^{6,7} However, their absolute configurations remained unresolved. In this study, the absolute configurations of compounds 2–5 were determined by computational methods. In addition, all the compounds were evaluated for their effects on intracellular Ca²⁺ influx, nitric oxide (NO) production, and human cancer cells.

RESULTS AND DISCUSSION

Compound 1 had the molecular formula C₃₀H₄₀O₅ by analysis of its HRESIMS, ¹³C NMR, and DEPT spectra. The IR absorption bands indicated the presence of hydroxy (3442 cm⁻¹), α,β-unsaturated carbonyl (1656 cm⁻¹), and olefinic (1618 cm⁻¹) functional groups. These results agreed well with the UV absorption band at 273 nm, representative of an α,β-unsaturated carbonyl group.⁸ The ¹³C NMR and DEPT spectra indicated the presence of 30 carbons. The similarity of the



carbon chemical shifts complicated structure elucidation. The NMR data of 1 inferred the presence of a sesquiterpenoid similar to 1b⁶ but distinct in that two CH₂OH groups were attached to C-13 and C-16 in 1 instead of the two CH₃ groups as in 1b. This conclusion was supported by the HMBC correlations between H-27/C-2, C-13, C-14, C-26 and H-28/C-15, C-16, C-17. The molecular structure of 1 was thus determined as shown.

Compound 1 is a rare sesquiterpenoid possessing an unusual hydrodecalenone-substituted tricyclic skeleton that is derived from the nonisoprenoid eremophilane sesquiterpenes. Previously only two analogues of 1 were isolated from the genus *Eremophila*; however their absolute configurations remained

Received: November 18, 2011

Published: May 23, 2012

unresolved. The correlations between H-11, H-12/Ha-1 and H-29, H-30/Ha-18 in **1** and between H-11/H-12 and H-29/H-30 observed in the ROESY spectrum of **1a** (the *O*-acetyl derivative of **1**) revealed the relative configurations of the stereogenic carbons at rings A, B, D, and E, as shown. The relative configuration of the C-ring chiral centers was difficult to assign due to the paucity of useful ROESY correlations. In this case, compound **1** was converted into its *O*-acetyl derivative, which yielded a good-quality crystal for X-ray diffraction studies using Cu radiation, which suggested the configuration of **1**, as illustrated below (Figure 1). The absolute configuration of **1** was thus assigned as 9*S*,10*R*,13*R*,16*S*,19*R*,20*S*.

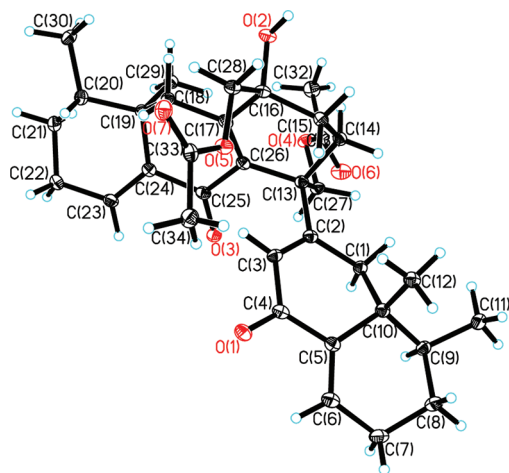


Figure 1. X-ray crystal structure showing the absolute configuration of **1a**.

Compound **2** had the same molecular formula as that of **1** by analysis of its HRESIMS, ^{13}C NMR, and DEPT spectra. The striking similarities of NMR data between compounds **1** and **2** inferred that they are isomers. The differences between the chemical shifts of the two compounds at C-15, C-16, C-17, C-26, and C-28 indicated that **2** is the C-16 epimer of **1**. This assumption was further confirmed on the basis of the correlations of H-11, H-12/Ha-1, H-29, H-30/Ha-18, H-11/H-12, and H-29/H-30, as well as weak ROESY correlations of H-29/H-27a, H-27b, H-28a, and H-28b in compound **2a**, which showed that the relative configurations of the stereogenic carbons at rings A, B, D, and E in **2** were identical to those of **1**. Because the crystals of **2** or its *O*-acetyl derivative (**2a**) could not be obtained, a computational approach was employed to determine the configuration of this substance. The ^{13}C NMR spectra of **1** and **2** were computed at the B3LYP/6-311++G(2d,p)//B3LYP/6-31+G(d) level.⁹ The relative error distributions of the computed and recorded spectra of **1** and **2**, illustrated in Figures 1 and 2 in the Supporting Information, were found to be lower than the maximum control of 8.0 ppm, which means that both structures were possible. Since the configuration of compound **1** was determined unambiguously by using X-ray diffraction methods, the assigned structure and configuration of **2** were considered to be highly reliable. The shift errors between the recorded and calculated ^{13}C NMR spectra of **1** and **2** were also determined, and, in most cases, the data were in good agreement (Supporting Information, Figure 2). Thus, the absolute configuration of **2** was assigned as 9*S*,10*R*,13*R*,16*R*,19*R*,20*S*.

Compound **3** was found to have the molecular formula $\text{C}_{30}\text{H}_{40}\text{O}_4$ by analysis of its HRESIMS spectrum, which displayed a quasi-molecular ion peak at m/z 463.2857 [$\text{M} - \text{H}$]⁻ (calcd 463.2848). The UV, IR, and NMR spectra of **3** were similar to those of **1**, indicating that these substances are closely related. Analysis of the spectroscopic data showed that CH (δ_{C} 46.3) in **3** replaces one oxygenated quaternary carbon (δ_{C} 72.8) in **1**, indicating that the OH group at C-16 in **1** is absent in **3**. This proposal agreed well with the observed $^1\text{H}-^1\text{H}$ COSY correlations between H-13/H-14/H-15/H-16 and the HMBC correlations between H-28/C-15, C-16, and C-17. The ROESY correlations of H-11/H-12 and H-29/H-30 were used to assign the relative configurations of stereocenters at rings A, B, D, and E. The ROESY correlations of H-14a/H-16/H-29 and H-14b/H-1a enabled assignment of the relative configuration of stereogenic carbons at ring C. This was confirmed by computational methods, which enabled the assignment of the absolute configuration of **3**. The electronic circular dichroism (ECD) spectrum of **3** was computed at the B3LYP/6-311++G(2d,p) level using the B3LYP/6-31+G(d)-optimized geometries.¹⁰ The computed ECD spectrum for the 9*S*,10*R*,13*R*,16*R*,19*R*,20*S* stereoisomer of **3** was compared to the recorded ECD spectrum (Figure 2), indicating that the

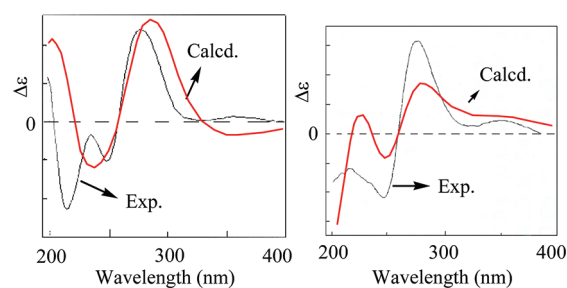


Figure 2. The computed and recorded ECDs for **3** (left) and **4** (right).

computed and experimental ECD spectra agreed well except for a red-shift in the ECD spectrum of **3**. Therefore, the absolute configuration of **3** was assigned as 9*S*,10*R*,13*R*,16*R*,19*R*,20*S*.

Compound **4** was obtained as a yellow, amorphous solid, and the HRESIMS displayed a quasi-molecular ion peak at m/z 447.2538 [$\text{M} - \text{H}$]⁻ (calcd for 447.2535), corresponding to the molecular formula $\text{C}_{29}\text{H}_{36}\text{O}_4$. The UV spectrum displayed an absorption band at 267 nm. The ^{13}C NMR spectrum showed 29 resonances, most of which occur at chemical shifts that are similar to those of **1** with the exception of a C-16 carbonyl group (δ_{C} 201.5) in **4**. This assignment was supported by the HMBC cross-peaks between H-14, H-15, H-18/C-16. Serious overlap among the proton signals made it difficult to interpret the ROESY correlations. The relative configurations of the stereocenters at rings A, B, D, and E of **4** were identical to those of **1** from a biogenetic point of view. The absolute configuration of **4** was established in the same manner as **3**, as shown by comparison of the computed and recorded ECD spectra (Figure 2), both showing strong positive Cotton effects at around 280 nm. Accordingly, the absolute configuration of **4** was determined as 9*S*,10*R*,13*R*,16*R*,19*R*,20*S*.

The molecular formula of **5** was deduced to be $\text{C}_{15}\text{H}_{22}\text{O}_2$ on the basis of analysis of its HRESIMS, ^1H and ^{13}C NMR (Table 3), and DEPT data. The NMR spectra of **5** were similar to those of **6**.¹¹ The $^1\text{H}-^1\text{H}$ COSY correlations between H-13/H-11/H-12 and HMBC correlations of H-8 (δ_{H} 5.95)/C-6, C-10, C-11, H-11/C-6, C-7, C-8 indicated the presence of a $\Delta^{7(8)}$

double bond in **5**, and the $\Delta^{11(13)}$ double bond in **6** was saturated in **5**. The ROESY interactions of H₃-14/H₃-15 in **5** suggested their vicinal disposition. The assignment of the configuration at C-11 of the conformationally flexible side chain is challenging. The calculated ECD spectrum of **5** (Figure 3)

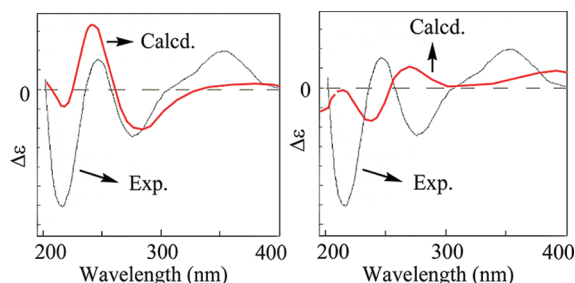


Figure 3. Computed and recorded ECDs for **5** with 11S (left) and 11R (right) configuration.

with 11R configuration differed significantly from the experimental spectrum. Finally, the optical rotation (OR) of **5**¹¹ was computed by using conformation searching with a MMFF94S force field, and low-energy conformations were used in optimizations at the B3LYP/6-31+G(d) level. The low-energy (0–2.5 kcal/mol) conformations were further used to calculate optical rotations, and Boltzmann statistics analysis was employed to calculate the overall OR. The computed OR for **5** with 11R configuration was +7.4 and for the 11S diastereoisomer was –14.6, the latter of which more closely matched the experimental OR value of –23.3 determined experimentally. Thus, the combined ECD and OR results suggest that **5** has an 11S configuration.

The five new compounds were accompanied by the known compound argutosine B (**6**)¹¹ in the extract of *I. arguta*.

Given the traditional uses of *I. arguta*, an ethnopharmacology-based strategy was applied to a biological screen. Argutosine B (**6**) was found to exhibit LPS-stimulated NO inhibition in RAW264.7 macrophages with an IC₅₀ value of 5.7 μM, using MG-132 (a proteasome inhibitor) as a positive control (IC₅₀ = 0.08 μM). These results suggested the potential applicability of **6** to the treatment of inflammation-related diseases. To exclude the possibility that the effect of **6** was influenced by its cellular toxicity, an MTT assay was performed in each experiment. The result demonstrated that **6** exhibited no cytotoxicity in RAW 264.7 macrophages at the concentrations of 0.04, 0.2, 1, 5, and 25 μM. Further, **6** displayed cytostatic activities toward HL-60 (IC₅₀ = 15.2 μM), SMMC-7721 (IC₅₀ = 34.1 μM), MCF-7 (IC₅₀ = 13.5 μM), and SW-480 (IC₅₀ = 15.6 μM) cancer cells, while all the other compounds were inactive (IC₅₀ > 40 μM).

Calcium influx and signaling have been implicated to be involved in a wide range of physiological and pathological processes. All the compounds were evaluated for their calcium-modulating activities via a calcium imaging assay. Compounds **1**, **2**, and **4** were found to significantly stimulate intracellular calcium levels in A549 cells with an HBSS buffer containing Ca²⁺ (Figure 4), indicating their role in calcium-dependent signal pathways. Investigations of the physiological consequences of calcium signaling induced by these substances are ongoing.

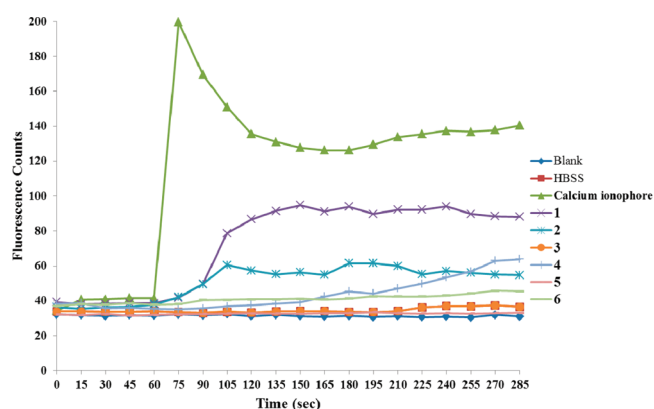


Figure 4. Stimulation by **1–6** (10 μM) of calcium signaling in A549 cells.

EXPERIMENTAL SECTION

General Experimental Procedures. Optical rotation measurements were made using a Horiba SEPA-300 polarimeter. UV spectra were recorded on a Shimadzu UV-2401PC spectrometer. IR spectra were measured using a Tensor 27 spectrometer with KBr pellets. NMR spectra were recorded on a Bruker AV-400 or DRX-500 or an Avance III 600 spectrometer with TMS as an internal standard. EIMS spectra were determined on a VG Autospec-3000 spectrometer. ESIMS and HRESIMS spectra were determined using an API QSTAR Pulsar 1 spectrometer. The X-ray data were collected on a Bruker AXS SMART APEX II CCD diffractometer. Silica gel (200–300 mesh; Qingdao Marine Chemical, Inc., People's Republic of China), MCI gel CHP 20P (75–150 μm; Mitsubishi Chemical, Co., Japan), RP-18 gel (40–63 μm; Daiso, Co., Japan), and Sephadex LH-20 (Amersham Biosciences, Sweden) were used for column chromatography. CD spectra were measured on a Chirascan instrument.

Plant Material. Whole plants of *I. arguta* were collected in July 2008 from Dongchuan County, Yunnan Province, People's Republic of China, and were identified by Mr. Bin Qiu of Yunnan Institute of Materia Medica. A voucher specimen (CHYX-0474) has been deposited at the Kunming Institute of Botany, Chinese Academy of Sciences.

Extraction and Separation. The dried whole plant powders of *I. arguta* (20 kg) were extracted three times with 95% EtOH (each 25 L, 48 h) at room temperature to give an extract (3 kg), which was suspended in H₂O and partitioned with petroleum ether, EtOAc, and *n*-BuOH (each 4 × 8 L). The EtOAc extract (75 g) was subjected to silica gel column chromatography (CHCl₃/MeOH, 1:0 to 0:1) to produce fractions A–F. Fraction B (7.3 g) was separated into fractions B1–B6 by MCI gel CHP 20P with MeOH/H₂O (40:60–100:0) as the eluent. Fraction B4 (1.1 g) was gel filtered over Sephadex LH-20 (MeOH), followed by a RP-18 column (MeOH/H₂O, 40:60–70:30), to give B4.4 (400 mg), which was further purified by silica gel eluted with CHCl₃/Me₂CO (40:1–5:1) to give compounds **5** (2.5 mg) and **6** (85 mg). Fraction B5 (1.2 g) was separated into fractions B5.1–B5.4 by Sephadex LH-20 (MeOH). Fraction B5.1 (250 mg) was purified by a RP-18 column using MeOH/H₂O (30:70–70:30), followed by preparative TLC developed with petroleum ether/Me₂CO (3:1), to afford **3** (10 mg). Fraction B6 (1.1 g) was fractionated by a RP-18 column (MeOH/H₂O, 40:60–70:30), followed by preparative TLC developed with petroleum ether/*n*-PrOH (6:1), to give **4** (13 mg). Fraction E (12.5 g) was divided into E1–E5 by MCI gel CHP 20P eluted with MeOH/H₂O (40:60–100:0). Fraction E3 (200 mg) was subjected to silica gel column chromatography (petroleum ether/Me₂CO, 2.5:0 to 1:1) and further purified via a RP-18 column (MeOH/H₂O, 60:40) to give **1** (20 mg) and **2** (5 mg).

Diincarvilone A (1): white, amorphous solid; $[\alpha]_D^{15} +60$ (c 0.13, MeOH); UV (MeOH) λ_{max} (log ϵ) 273 (4.24), 199 (3.87) nm; CD (MeOH) $\Delta\epsilon_{198} +3.30$, $\Delta\epsilon_{217} -9.04$, $\Delta\epsilon_{269} +10.59$, $\Delta\epsilon_{347} +0.42$; IR (KBr) ν_{max} 3442, 2961, 2925, 2876, 1656, 1618, 1461, 1422, 1384,

1370, 1334, 1287, 1129, 1049, 882, 599 cm^{-1} ; ^1H and ^{13}C NMR data, see Tables 1 and 2; ESIMS (negative) m/z 515 $[\text{M} + \text{Cl}]^-$; HRESIMS (negative) m/z 515.2568 $[\text{M} + \text{Cl}]^-$ (calcd for $\text{C}_{30}\text{H}_{40}\text{O}_5\text{Cl}$, 515.2564).

Table 1. ^1H NMR Data of Compounds 1–4 (500 MHz)

	1	2	3	4
position	δ_{H}^a (J in Hz)	δ_{H}^a (J in Hz)	δ_{H}^b (J in Hz)	δ_{H}^a (J in Hz)
1a	2.66, d (17.4)	2.64, d (17.4)	2.68, d (17.3)	2.67, d (17.4)
1b	2.25, overlap	2.28, overlap	2.29, dd (17.3, 2.4)	2.30, overlap
3	5.72, d (2.5)	5.66, d (2.4)	5.68, d (2.6)	5.62, d (2.6)
6	6.74, t (3.7)	6.76, dd (7.3, 3.5)	6.60, t (3.8)	6.79, t (3.8)
7	2.25, overlap	2.28, overlap	2.21, overlap	2.30, overlap
8	1.54, overlap	1.52, overlap	1.47, overlap	1.54, overlap
9	1.69, overlap	1.75, tq (12.3, 3.1)	1.69, m	1.75, tq (12.3, 3.1)
11	0.99, d (6.8)	1.03, d (6.9)	0.98, d (6.8)	1.03, d (6.9)
12	0.95, s	0.96, s	0.93, s	0.98, s
14a	2.25, overlap	2.18, dt (14.6, 2.9)	1.92, m	2.52, overlap
14b	1.67, m	1.52, overlap	1.81, dt (13.2, 3.3)	2.09, dt (5.5, 3.1)
15a	2.05, dt (14.2, 2.8)	2.11, dt (14.4, 2.9)	1.71, m	2.52, overlap
15b	1.57, m	1.64, dt (14.4, 3.4)		
16			2.38, m	
18a	2.95, d (17.1)	2.89, d (17.5)	2.62, d (17.2)	3.14, d (17.9)
18b	2.25, overlap	2.28, overlap	2.44, d (17.2)	2.02, d (17.9)
20	1.69, overlap	1.67, overlap	1.64, m	1.69, tq (12.3, 3.1)
21	1.54, overlap	1.52, overlap	1.47, overlap	1.54, overlap
22	2.25, overlap	2.28, overlap	2.21, overlap	2.30, overlap
23	6.77, t (3.8)	6.76, dd (7.3, 3.5)	6.68, t (3.8)	6.93, t (3.8)
27a	4.13, d (10.0)	4.15, d (9.7)	4.08, dd (9.7, 6.3)	4.31, d (9.7)
27b	3.76, d (10.0)	3.65, d (9.7)	3.69, br d (9.3)	3.73, d (9.7)
28a	3.69, d (10.9)	3.75, d (11.6)	3.84, d (11.1)	1.02, overlap
28b	3.36, d (10.9)	3.66, d (11.6)	3.69, br d (9.3)	
29	1.05, s	1.00, s	1.03, s	1.02, overlap
30	1.02, d (6.8)	1.02, d (6.9)	0.98, d (6.8)	

^aIn methanol- d_4 . ^bIn acetone- d_6 .

Diincarvilone B (2): white, amorphous solid; $[\alpha]_{\text{D}}^{15} +20.9$ (c 0.2, MeOH); UV (MeOH) λ_{max} (log ϵ) 276 (4.13), 199 (3.87) nm; CD (MeOH) $\Delta\epsilon_{199} +5.53$, $\Delta\epsilon_{213} -2.35$, $\Delta\epsilon_{251} -5.79$, $\Delta\epsilon_{280} +4.27$, $\Delta\epsilon_{350} +0.63$; IR (KBr) ν_{max} 3438, 2958, 2924, 2857, 1656, 1620, 1461, 1423, 1376, 1334, 1284, 1202, 1049, 977, 578 cm^{-1} ; ^1H and ^{13}C NMR data, see Tables 1 and 2; ESIMS (negative) m/z 515 $[\text{M} + \text{Cl}]^-$; HRESIMS (negative) m/z 515.2569 $[\text{M} + \text{Cl}]^-$ (calcd for $\text{C}_{30}\text{H}_{40}\text{O}_5\text{Cl}$, 515.2564).

Diincarvilone C (3): white, amorphous solid; $[\alpha]_{\text{D}}^{15} +37.7$ (c 0.13, MeOH); UV (MeOH) λ_{max} (log ϵ) 274 (4.03), 199 (3.74) nm; CD (MeOH) $\Delta\epsilon_{199} +3.02$, $\Delta\epsilon_{215} -5.85$, $\Delta\epsilon_{248} -2.64$, $\Delta\epsilon_{278} +6.14$, $\Delta\epsilon_{354} +0.31$; IR (KBr) ν_{max} 3432, 2959, 2925, 2875, 1656, 1619, 1461, 1371, 1284, 1045, 883, 586 cm^{-1} ; ^1H and ^{13}C NMR data, see Tables 1 and 2; ESIMS (negative) m/z 463 $[\text{M} - \text{H}]^-$; HRESIMS (negative) m/z 463.2857 $[\text{M} - \text{H}]^-$ (calcd for $\text{C}_{30}\text{H}_{39}\text{O}_4$, 463.2848).

Diincarvilone D (4): yellow gum; $[\alpha]_{\text{D}}^{15} +39.1$ (c 0.3, MeOH); UV (MeOH) λ_{max} (log ϵ) 267 (4.17), 202 (4.08) nm; CD (MeOH) $\Delta\epsilon_{245} +5.83$, $\Delta\epsilon_{276} +7.17$, $\Delta\epsilon_{350} +0.86$; IR (KBr) ν_{max} 3439, 2959, 2923, 2855, 1656, 1626, 1460, 1377, 1257, 1166, 1056, 976, 577 cm^{-1} ; ^1H and ^{13}C NMR data, see Tables 1 and 2; ESIMS (negative) m/z 447

Table 2. ^{13}C NMR Data of Compounds 1–4 (100 MHz)

	1	2	3	4
position	δ_{C}^a	δ_{C}^a	δ_{C}^b	δ_{C}^a
1	39.9 CH ₂	39.9 CH ₂	39.5 CH ₂	40.2 CH ₂
2	167.4 qC	169.0 qC	164.9 qC	164.9 qC
3	126.5 CH	125.3 CH	127.2 CH	126.5 CH
4	190.7 qC	190.8 qC	187.7 qC	190.3 qC
5	142.7 qC	142.5 qC	142.6 qC	142.3 qC
6	136.9 CH	137.3 CH	133.8 CH	137.8 CH
7	27.2 CH ₂	27.3 CH ₂	26.6 CH ₂	27.4 CH ₂
8	27.3 CH ₂	27.1 CH ₂	27.1 CH ₂	27.5 CH ₂
9	40.9 CH	40.9 CH	40.4 CH	40.9 CH
10	40.1 qC	39.7 qC	39.2 qC	40.0 qC
11	15.9 CH ₃	15.9 CH ₃	15.7 CH ₃	15.9 CH ₃
12	19.8 CH ₃	19.7 CH ₃	19.7 CH ₃	20.0 CH ₃
13	50.6 qC	50.3 qC	50.1 qC	51.3 qC
14	26.4 CH ₂	27.8 CH ₂	29.7 CH ₂	29.4 CH ₂
15	29.7 CH ₂	27.5 CH ₂	22.2 CH ₂	34.6 CH ₂
16	72.8 qC	74.9 qC	46.3 CH	201.5 qC
17	158.8 qC	162.2 qC	158.9 qC	147.5 qC
18	38.3 CH ₂	39.8 CH ₂	42.5 CH ₂	35.6 CH ₂
19	38.6 qC	38.9 qC	37.9 qC	38.2 qC
20	41.0 CH	40.9 CH	40.3 CH	40.8 CH
21	27.3 CH ₂	27.1 CH ₂	26.9 CH ₂	27.2 CH ₂
22	27.1 CH ₂	27.2 CH ₂	26.4 CH ₂	27.1 CH ₂
23	137.1 CH	137.1 CH	135.0 CH	139.5 CH
24	143.2 qC	143.3 qC	142.6 qC	142.9 qC
25	188.7 qC	188.1 qC	186.6 qC	189.4 qC
26	137.4 qC	135.6 qC	136.6 qC	148.5 qC
27	66.4 CH ₂	65.6 CH ₂	66.6 CH ₂	65.9 CH ₂
28	67.3 CH ₂	65.3 CH ₂	63.5 CH ₂	16.0 CH ₃
29	19.4 CH ₃	19.2 CH ₃	19.2 CH ₃	19.4 CH ₃
30	15.8 CH ₃	15.8 CH ₃	15.9 CH ₃	

^aIn methanol- d_4 . ^bIn acetone- d_6 .

$[\text{M} - \text{H}]^-$; HRESIMS (negative) m/z 447.2538 $[\text{M} - \text{H}]^-$ (calcd for $\text{C}_{29}\text{H}_{35}\text{O}_4$, 447.2535).

Incarvilone A (5): colorless gum; $[\alpha]_{\text{D}}^{20} -23.3$ (c 0.1, MeOH); UV (MeOH) λ_{max} (log ϵ) 252 (3.93), 200 (3.67) nm; CD (MeOH) $\Delta\epsilon_{196} +1.45$, $\Delta\epsilon_{217} -3.08$, $\Delta\epsilon_{246} +0.79$, $\Delta\epsilon_{276} -1.24$, $\Delta\epsilon_{349} +0.99$; IR (KBr) ν_{max} 3432, 2962, 2925, 2876, 1656, 1631, 1461, 1422, 1383, 1283, 1047, 975, 583 cm^{-1} ; ^1H and ^{13}C NMR data, see Table 3; ESIMS (negative) m/z 269 $[\text{M} + \text{Cl}]^-$; HRESIMS (negative) m/z 269.1316 $[\text{M} + \text{Cl}]^-$ (calcd for $\text{C}_{15}\text{H}_{22}\text{O}_2\text{Cl}$, 269.1308).

Crystallographic data for compound **1a**: $\text{C}_{34}\text{H}_{44}\text{O}_7$, $M_r = 564.69$, orthorhombic, space group $P2_12_12_1$, $a = 9.1073(2)$ Å, $b = 16.7095(3)$ Å, $c = 19.7397(4)$ Å, $V = 3003.96(10)$ Å³, $Z = 4$, $D_{\text{calcd}} = 1.249$ g cm^{-3} , crystal size $0.28 \times 0.45 \times 0.52$ mm³, $F(000) = 1216$. The final R_1 value is 0.0447 ($wR_2 = 0.1366$) for 5123 reflections [$I > 2\sigma(I)$]. Flack structure parameter: 0.10 (18).

The crystallographic data for compound **1a** have been deposited with the Cambridge Crystallographic Data Centre (deposit number CCDC 846486). Copies of the data can be obtained, free of charge, on application to the Director, CCDC, 12 Union Road, Cambridge CB2 1EZ, UK (fax: +44-(0)1223-336033) or e-mail: deposit@ccdc.cam.ac.uk.

Preparation of 1a and 2a. Diincarvilone A or B (each 1.5 mg) was dissolved in freshly distilled dry pyridine (2 mL), and Ac_2O (1.0 mL) was added. The mixture was stirred for 12 h at room temperature. The reaction mixture was diluted with H_2O (2 mL) and extracted with CH_2Cl_2 (3×3 mL). The CH_2Cl_2 extracts were concentrated in vacuo to give a residue, which was subjected to preparative TLC ($\text{CHCl}_3/\text{Me}_2\text{CO}$, 20:1) to give compound **1a** (1.0 mg) or **2a** (1.0 mg).

Inhibition of Nitric Oxide Production Assay. The assay was performed as described previously.⁸ Wells with DMSO were used as a

Table 3. NMR Spectroscopic Data for 5^a

position	δ_{H}^b (J in Hz)	δ_{C}^b
1	6.78, t-like (3.6)	136.9, CH
2	2.28, overlap	27.0, CH ₂
3	1.53, m	27.2, CH ₂
4	1.70, m	40.9, CH
5		39.7, qC
6a	2.55, d (17.5)	42.5, CH ₂
6b	2.28, overlap	
7		168.7, qC
8	5.95, s	125.2, CH
9		190.9, qC
10		142.8, qC
11	2.49, m	45.6, CH
12	3.60, m	65.7, CH ₂
13	1.11, d (6.8)	15.2, CH ₃
14	1.01, d (6.7)	15.8, CH ₃
15	0.98, s	19.8, CH ₃

^a500 MHz for ¹H, 100 MHz for ¹³C. ^bIn methanol-d₄.

negative control, and MG-132 was used as a positive control. Cytotoxicity was determined by the MTT assay as described.¹³

Cytostatic Assay. The cytostatic assay was performed using the MTT method, as reported previously, with slight modification.^{14,15} Briefly, human tumor cells were seeded into 96-well plates and permitted to adhere for 12 h before drug addition. Suspended cells were seeded immediately before drug addition with an initial density of (1–2) × 10⁵ cells/mL. Each cell line was incubated with different concentrations of the compounds for 48 h. Cisplatin and taxol were used as positive controls. Cell viability was measured, and IC₅₀ values were calculated.

Calcium Imaging Assay. The calcium imaging assay was performed by an automated, cell-based fluorescence-imaging system (Arrayscan) by a previously reported method with slight modification.^{16,17} The adenocarcinomic human alveolar basal epithelial cells A549 were seeded in 96-well plates with 0.5 × 10⁴ cells per well and incubated for 12 h. Then, the cells were stained with Fluo-4 AM for 30 min and subsequently washed three times with HBSS buffer. Calcium images of cells in HBSS buffer were acquired and analyzed using an ArrayScan VTI HCS Reader (Cellomics, Thermo Scientific, Pittsburgh, PA, USA).

■ ASSOCIATED CONTENT

📄 Supporting Information

1D and 2D NMR spectra and MS of the new compounds, X-ray crystallographic data in CIF format for compound 1a, quantum calculations for compounds 1 and 2. This material is available free of charge via the Internet at <http://pubs.acs.org>.

■ AUTHOR INFORMATION

Corresponding Author

*Tel/Fax: 86-871-5223048. E-mail: yxcheng@mail.kib.ac.cn; hjzhu@mail.kib.ac.cn.

Notes

The authors declare no competing financial interest.

■ ACKNOWLEDGMENTS

This work was financially supported by the Open Research Fund of the State Key Laboratory Breeding Base of Systematic Research, Development and Utilization of Chinese Medicine Resources and grants of the Top Talent Recruitment Program of Yunnan Province (2009C1120 and 20080A007) and 973 Program (2009CB522300).

■ REFERENCES

- (1) Wang, W. C.; Pan, K. Y.; Zhang, Z. Y.; Li, Z. Y.; Tao, D. D.; Yin, W. Q. *Flora of China*; Science Press: Beijing, 1990; Vol. 69, pp 34–36.
- (2) Nakamura, M.; Chi, Y. M.; Yan, W. M.; Nakasugi, Y.; Yoshizawa, T.; Irino, N.; Hashimoto, F.; Kinjo, J.; Nohara, T.; Sakurada, S. *J. Nat. Prod.* **1999**, *62*, 1293–1294.
- (3) Fu, J. J.; Jin, H. Z.; Shen, Y. H.; Qin, J. J.; Wang, Y.; Huang, Y.; Zeng, Q.; Zhang, W. D. *Chem. Biodivers.* **2009**, *6*, 818–826.
- (4) Yu, Z. W.; Zhu, H. Y.; Yang, X. S.; Sun, Q. Y.; Hao, X. J. *China J. Chin. Materia Med.* **2005**, *30*, 1335–1338.
- (5) Fu, J. J.; Shen, Y. H.; Jin, H. Z.; Xu, W. Z.; Zhang, W. D. *Nat. Prod. Res. Dev.* **2007**, *19*, 343–345.
- (6) Lewis, D. E.; Massy-Westropp, R. A.; Ingham, C. F.; Wells, R. J. *Aust. J. Chem.* **1982**, *35*, 809–826.
- (7) Beattie, K. D.; Waterman, P. G.; Forster, P. I.; Thompson, D. R.; Leach, D. N. *Phytochemistry* **2011**, *72*, 400–408.
- (8) Zhou, X. J.; Chen, X. L.; Li, X. S.; Su, J.; He, J. B.; Wang, Y. H.; Li, Y.; Cheng, Y. X. *Bioorg. Med. Chem. Lett.* **2011**, *21*, 373–376.
- (9) (a) Zhu, H. J. *Modern Organic Stereochemistry*; Science Press: Beijing, 2009. (b) Pu, J. X.; Huang, S. X.; Ren, J.; Xiao, W. L.; Li, L. M.; Li, R. T.; Li, L. B.; Liao, T. G.; Lou, L. G.; Zhu, H. J.; Sun, H. D. *J. Nat. Prod.* **2007**, *70*, 1706–1711. (c) Hua, Y.; Ren, J.; Chen, C. X.; Zhu, H. J. *Chem. Res. Chin. Univ.* **2007**, *23*, 592–596. (d) Frisch, M. J.; Trucks, G. W.; Schlegel, H. B.; et al. *Gaussian 03 User's Reference*; Gaussian Inc.: Carnegie, PA, USA, 2003.
- (10) (a) Specht, K. M.; Nam, J.; Ho, D. M.; Berova, N.; Kondru, R. K.; Beratan, D. N.; Wipf, P.; Pittman, R. A., Jr; Kahne, D. *J. Am. Chem. Soc.* **2001**, *123*, 8961–8966. (b) Ren, J.; Jiang, J. X.; Li, L. B.; Liao, T. G.; Tian, R. R.; Chen, X. L.; Jiang, S. P.; Pittman, C. U., Jr; Zhu, H. J. *Eur. J. Org. Chem.* **2009**, 3987–3991. (c) Lu, Z. Y.; Zhu, H. J.; Fu, P.; Wang, Y.; Zhang, Z. H.; Lin, H. P.; Liu, P. P.; Zhuang, Y. B.; Hong, K.; Zhu, W. M. *J. Nat. Prod.* **2010**, *73*, 911–914. (d) Ren, J.; Zhu, H. J. *Chem. J. Chin. Univ.* **2009**, *30*, 1907–1918.
- (11) Fu, J. J.; Qin, J. J.; Zeng, Q.; Huang, Y.; Jin, H. Z.; Zhang, W. D. *Chem. Pharm. Bull.* **2010**, *58*, 1263–1266.
- (12) (a) Taniguchi, T.; Martin, C.; Monde, K.; Nakanishi, K.; Berova, N.; Overman, L. *J. Nat. Prod.* **2009**, *72*, 430–432. (b) Stephens, P. J.; Pan, J. J.; Devlin, F. J.; Urbanova, M.; Julinek, O.; Hajicek, J. *Chirality* **2008**, *20*, 454–470. (c) Zhao, S. D.; Shen, L.; Luo, D. Q.; Zhu, H. J. *Curr. Org. Chem.* **2011**, *15*, 1843–1862.
- (13) Israf, D. A.; Khaizurin, T. A.; Syahida, A.; Lajis, N. H.; Khozirah, S. *Mol. Immunol.* **2007**, *44*, 673–679.
- (14) Mossmann, T. J. *Immunol. Methods* **1983**, *65*, 55–63.
- (15) Alley, M. C.; Scudiero, D. A.; Monks, A.; Hursey, M. L.; Czerwinski, M. J.; Fine, D. L.; Abbott, B. J.; Mayo, J. G.; Shoemaker, R. H.; Boyd, M. R. *Cancer Res.* **1988**, *48*, 589–601.
- (16) Gryniewicz, G.; Poenie, M.; Tsien, R. Y. *J. Biol. Chem.* **1985**, *260*, 3440–3450.
- (17) Schlag, B. D.; Lou, Z.; Fennell, M.; Dunlop, J. J. *Pharmacol. Exp. Ther.* **2004**, *310*, 865–870.